運輸省港湾技術研究所 (30th Anniversary Issue)

港湾技術研究所報告

REPORT OF THE PORT AND HARBOUR RESEARCH INSTITUTE

MINISTRY OF TRANSPORT

VOL. 31 NO. 5 MAR. 1993

NAGASE, YOKOSUKA, JAPAN

港湾技術研究所報告 (REPORT OF P.H.R.I.)

第31巻　第5号 (Vol. 31, No. 5) 1993年 3月 (Mar. 1993)

目　次 (CONTENTS)

REPORT OF THE PORT AND
HARBOUR RESEARCH INSTITUTE
Vol. 31, No. 5 (Mar. 1993)

8. Analysis of Liquefaction Induced Damage to Sheet Pile Quay Walls

Susumu IAI*
Tomohiro KAMEOKA**

Synopsis

In order to study the effects of liquefaction on quay walls during earthquakes, effective stress analyses are conducted on the field performance of two quay walls during an earthquake. The quay walls are of anchored steel sheet piles. Though the cross sections were similar to each other and the locations were adjacent to each other, one quay wall suffered serious damage while the other did not.

The effective stress model used in the analysis consists of a multiple shear mechanism defined in strain space. The model has the capability to represent essential features in the cyclic behavior of sand such as the effects of rotation of principal stress axis directions. For estimating the model parameters, soils were taken from the site for laboratory tests. The record of the earthquake motion was recovered from the site and digitized for the analysis.

Results of the finite element analysis are basically consistent with the observed performance of the quay walls; the model demonstrates the potential ability to differentiate between serious large deformations (i.e. damage) from negligibly small deformations (i.e. no damage) in similar types of sheet pile quay walls.

Key Words: dynamic, earthquake, finite element method, harbour, liquefaction, plasticity, retaining wall, sand, sheet pile wall

* Chief, Geotechnical Earthquake Engineering Laboratory, Structural Engineering Division
** Member, Geotechnical Earthquake Engineering Laboratory, Structural Engineering Division

港湾技術研究所報告
第31巻 第5号 (1992.12)

8. 液状化による矢板式岸壁の地震時被害の数値解析

井合 進*・亀岡知弘**

要 旨

本研究では，液状化が矢板式岸壁に与える影響を検討するため，矢板式岸壁の地震時挙動を有限要素法により解析した。解析の対象とした岸壁は控え工で支持された鋼矢板式の二つの岸壁である。両岸壁は互いに近接しており，その構造断面も同様であったが，一方は著しい地震被害を受けたのに対して，他方は無被害であった。両者には，地盤の密度に相違があったことが認められる。

解析に用いた土のモデルは，ひずみ空間で定義された多重せん断機構に基づくものである。このモデルは，主応力軸の回転の影響をはじめとして，繰返し載荷時の砂の種々の力学的挙動を表現することができる。解析に必要なパラメーターを決定するために，現地から砂を採取して室内試験を行った。また，解析に用いる入力地震動として，現地で記録された地震動の記録の数字化を行った。

解析の結果，被害および無被害岸壁の実際の地震時挙動と一致する結果が得られ，これにより，本モデルの矢板岸壁に対する適用性が確認された。

キーワード：液状化／港湾／地震／砂／塑性／矢板壁／有限要素法／擁壁

* 構造部地盤震動研究室長

** 構造部地盤震動研究室

Contents

1. Introduction

Past case histories during earthquakes show that quay walls often suffer significant damage if liquefaction occurs in the backfill and foundation soils. Some of the most typical examples are those observed during the Niigata Earthquake of 1964 (Ministry of Transport, 1965). Since then, extensive efforts have been made in developing methods to evaluate liquefaction susceptibility of soils and, as a result, practical means are now available to identify the conditions which lead to the occurrence of liquefaction. However, methods to evaluate effects of liquefaction on quay walls are yet to be developed.

Among the various types of retaining structures, the seismic performance of retaining structures backfilled with dry sand is relatively well understood based on the Mohr-Coulomb's failure criterion and the Newmark's sliding block concept. The recent developments in this subject can be found in the state-of-the-art report by Whitman (1991). When the sand is saturated with water, as in waterfront structures, the effect of pore water pressure becomes predominant and complicates the performance of retaining structures. Towhata and Islam (1987) offered a simplified method to incorporate the effect of pore water pressure into the sliding block concept. The method may be useful if reasonable engineering judgements are used in determining the level of excess pore water pressure and other relevant factors. Many laboratory data indicate, however, that the pore water pressure will not generally remain constant once deformation is induced in the sand nor will the deformation in the saturated sand generally be induced in such a mode of the sliding blocks as often observed in the dry sand. Effective stress analysis may be the only means for taking the complicated behavior of sand into account. In particular, a model consisting of a multiple shear mechanism (Iai et al., 1992a and b) offers the prospect of taking into account the essential features of sand under cyclic loading.

In May 1983, the Nihonkai Chubu Earthquake of magnitude 7.7 hit the northern part of Japan. The earthquake caused damage to quay walls at Akita Port located about 100 km from the epicenter. Many sand boils were observed at the quay walls. In the vicinity of one of the damaged quay walls, a quay wall survived without damage. The cross section of this wall was similar to that of the damaged quay wall, but no sand boils were observed. This case history provided a good opportunity to examine the capability of the aforementioned effective stress model to predict the effects of earthquakes on quay walls.

The present paper begins with a fairly comprehensive description of the case history. The paper then moves on to the analysis. Through the course of the analysis, various approximations and assumptions have to be made on such items as the initial conditions, the permeability of sand, the frictions between soil and structures, the two or three dimensional nature of the earthquake motions, etc. Discussions will be presented for examining the effects of those approximations in the final part of the paper in an attempt to identify what can be learned from the results of the analysis.

2. Akita Port and Earthquake Motion

The epicenter of the 1983 Nihonkai Chubu Earthquake was located in the Japan Sea, called 'Nihonkai' in Japanese, as shown in **Fig. 1**. The seismic fault, shown by the broken lines in **Fig. 1(b)**, dipped about 30 degrees in the east direction. With the

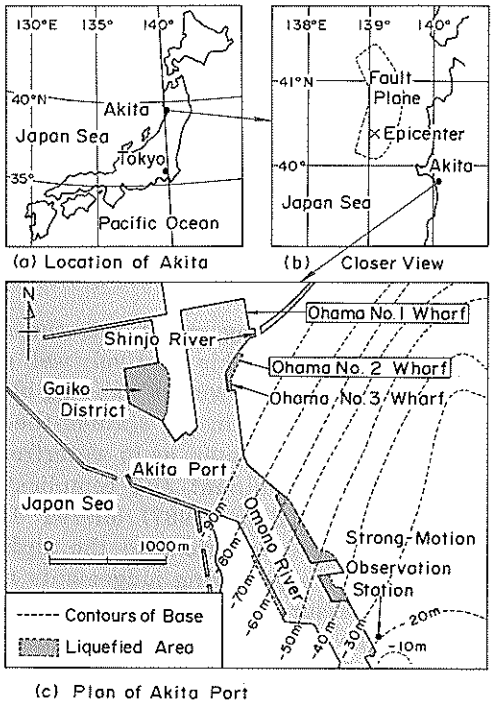

Fig. 1 Fault of the 1983 Nihonkai-Chubu Earthquake and liquefaction at Akita Port

shallow focal depth of 14 km, the earthquake caused Tsunami, killing 100 people.

As shown in **Fig. 1(c)**, Akita Port is situated at the estuaries of the Omono and the Shinjo Rivers. Most of the quay walls were constructed along the Omono River with a backfilling method. Most of them suffered damage due to liquefaction in the backfill sand during the earthquake. The quay walls to be analyzed in the present study are located at Ohma No. 2 Wharf where sand boils were observed and at Ohama No. 1 Wharf where no sand boils were observed. These wharves are located near the estuary of the Shinjo River as shown in the same figure.

About 2.5 km south east of these wharves, a strong motion accelerograph was installed at the location shown in the lower right corner of **Fig. 1(c)**. This is one of the stations deployed under the strong motion observation network of the Port and Harbour Research Institute in operation since 1963 (Kurata and Iai, 1990). The maximum accelerations recorded at Akita Port were 219, 235 and 54 Gals in NS, EW and UD directions.

The ground below the accelerograph, as shown in **Fig. 2**, consists of a layer of loosely deposited coarse and fine sands with thickness of about six meters and alternating layers of sandy gravel and gravel mixed with sands of about ten meters in thickness, below which lies the base of tertiary origin for the entire area of Akita Port. Contour lines of the depth of the base (Kano, 1965) are shown in **Fig. 1(c)** with the broken lines, indicating the accelerograph is located close to the shallowest part of the base. The soil deposit at the accelerograph site did not liquefy during the earthquake and thereby the earthquake motion recovered from the accelerograph was not affected by the soil liquefaction occurring in other parts of the area in Akita

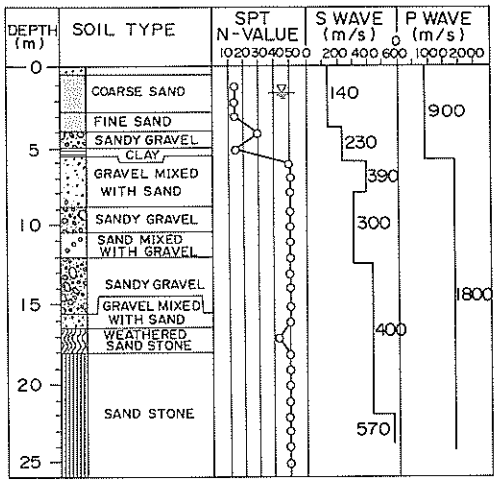

Fig. 2 Ground condition at the strong-motion observation station at Akita Port

Port. The recorded time histories of the earthquake motion were digitized and corrected for the instrument response of the accelerograph through the procedure developed by one of the authors and his colleagues (Iai et al., 1978). The accelerograph was of SMAC-B2 type commonly deployed in Japan. The corrected time histories are shown in **Fig. 3** (Kurata et al., 1983).

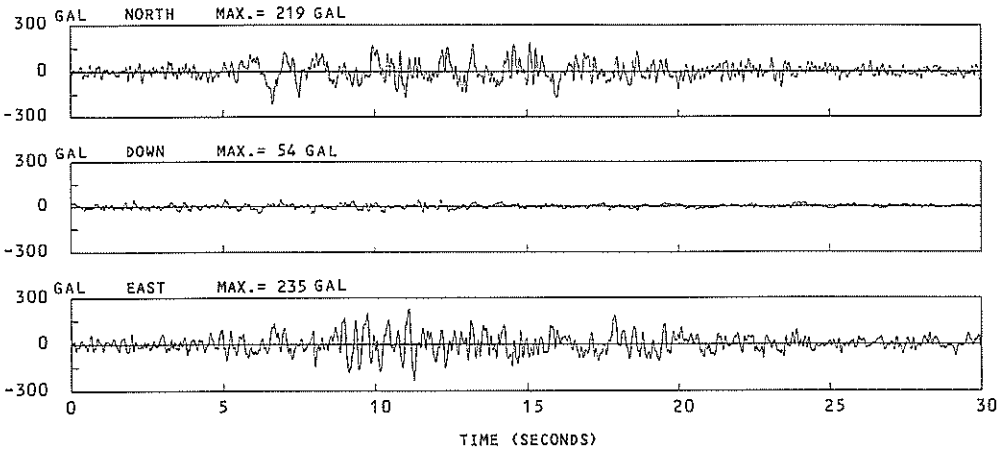

Fig. 3 Recorded earthquake motion at Akita Port

3. Damaged Quay Wall

At the time of the earthquake, the quay wall at Ohama No. 2 Wharf had such a cross section as shown in **Fig. 4**. As indicated in this figure, the quay wall was constructed with a backfilling method. The earthquake left sand boils at the quay wall, as mentioned earlier, and induced such deformations as shown in the same figure with the broken lines. An eyewitness, a truck driver who had narrowly escaped from

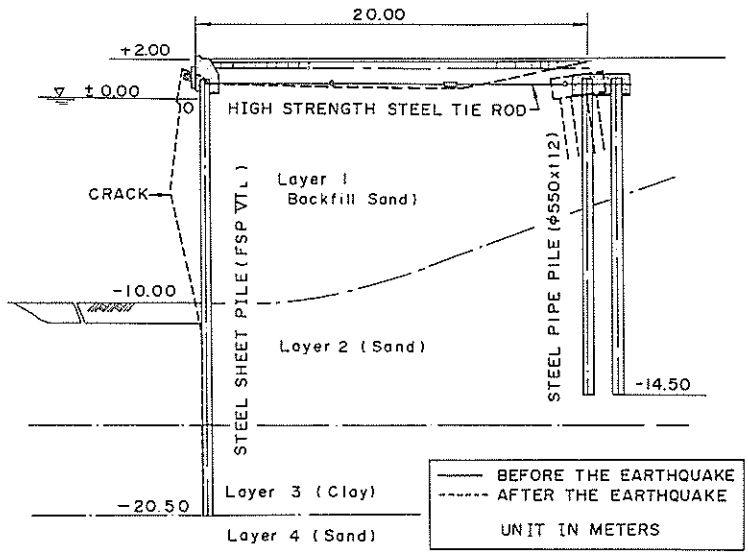

Fig. 4 Cross section of a quay wall at Ohama No. 2 Warf

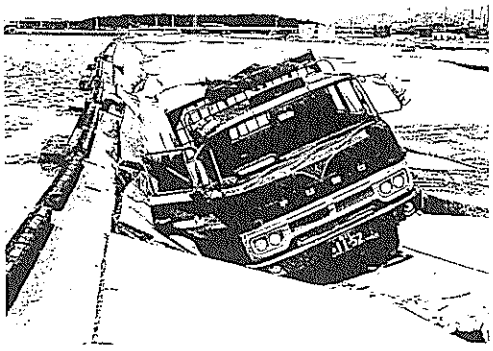

Photo. 1 Damage at Ohama No. 2 Wharf (courtesy of Akita Prefecture)

Ohama No. 2 Wharf shown in **Photo. 1**, identified that the quay wall gradually deformed during the earthquake (Tsuchida et al., 1985).

The deformations in the sheet pile and the anchor, plotted along the face line of the quay wall, are shown in **Fig. 5**. In this figure, the typical deformed cross sections are shown in **Fig. 5(a)** with the alphabets indicating the locations shown at the top row in **Fig. 5(b)**.

The quay wall at Ohama No. 2 Wharf consists of four sections as shown in **Fig. 5(b)**; the sections A and B and the approaches at both ends. The cross section shown earlier in **Fig. 4** is of section A but those of section B and the approaches are slightly different from this. The horizontal displacements at the top of the sheet pile wall, shown in the top row in **Fig. 5(b)**, are obviously constrained by the structures at the approaches at both ends of Ohama No. 2 Wharf. The dent shown in the second row in **Fig. 5(b)** at the left end of section B was due to the effect of the truck shown in **Photo. 1**.

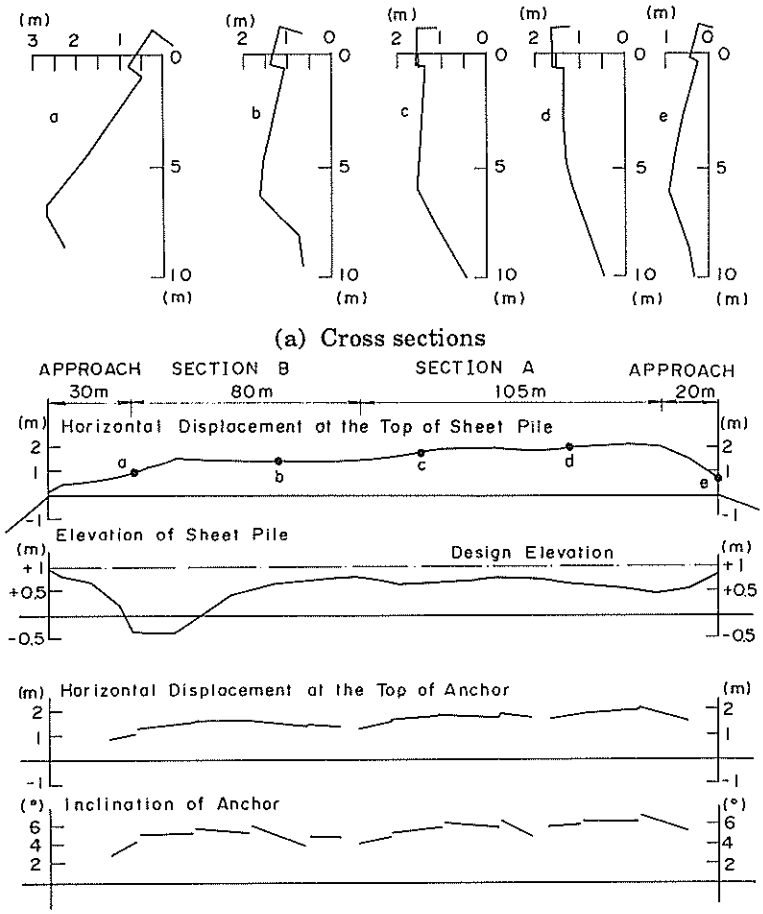

(a) Cross sections

(b) Distribution along the face line

Fig. 5 Deformation along the face line at Ohama No. 2 Warf

Since section A reveals relatively uniform two dimensional deformation, this section will be analyzed in the present study based on the two dimensional analysis model. The horizontal displacements at the top of the sheet pile in section A range from about 1.1 to 1.8 meters. The settlements at the middle part of the apron, which are indicated by the broken lines in **Fig. 4**, are about 1.4 meters, being almost the same as the horizontal displacements of the sheet pile wall.

The displacements at the top of the sheet pile wall are evidently associated with those of the anchor piles as shown in the third row in **Fig. 5(b)**; the anchors were pulled by the sheet piles towards the sea, accordingly inclined, as shown in the fourth row in **Fig. 5(b)**, presumably due to the reduced resistance in the liquefied backfill sand.

Ohama No. 2 Wharf consisted of such soil layers as shown in **Fig. 6** with the grain size accumulation curves of soils shown in **Fig. 7**. The upper layer of medium sand with the mean diameter D_{50} of about 0.15 mm is originally a part of the deposit from the Shinjo River and dredged from the sea bottom for the backfilling. The lower layer

of fine sand with D_{50} of about 0.4 mm is a deposit from the Omono River.

An in-situ velocity logging with a down hole method was obtained at Ohama No. 3 Wharf, which is adjacent to Ohama No. 2 Wharf. The location is shown in **Fig. 1(c)**. The velocity logging, shown in **Fig. 8**, will be used as a reference for estimating the in-situ elastic shear modulus of the ground at Ohama No. 2 Wharf. It will also be used for Ohama No. 1 Wharf to be described in the next chapter.

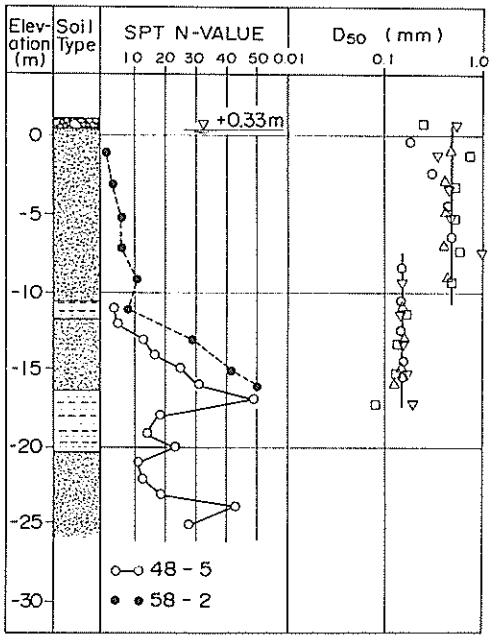

Fig. 6 Ground conditions at Ohama No. 2 Warf

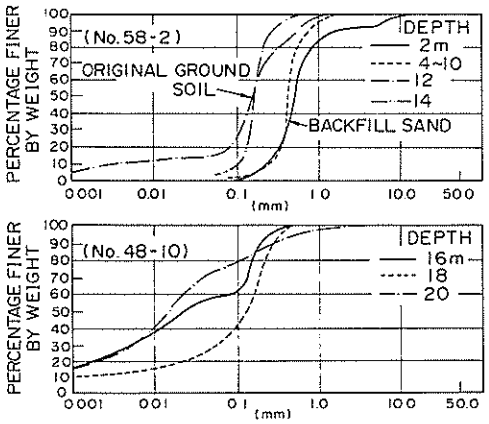

Fig. 7 Grain size accumulation curves of soils at Ohama No. 2 Wharf

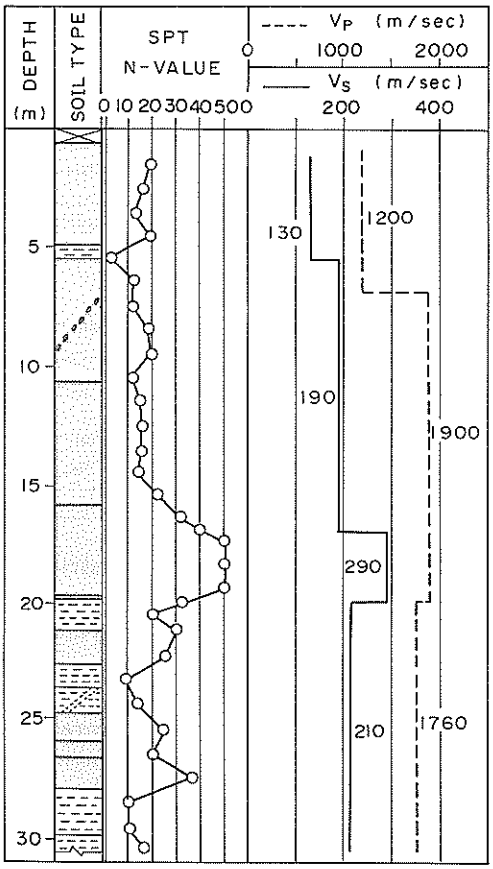

Fig. 8 In-situ velocity logging at Ohama No. 3 Wharf

4. Quay Wall Without Damage

The quay wall at Ohama No. 1 Wharf had a cross section similar to that at Ohama No. 2 Wharf as shown in **Fig. 9.** In particular, the type of the sheet pile wall and the water depth of the quay wall at Ohama No. 1 Wharf were exactly the same as those at Ohama No. 2 Wharf. The ground consisted of quaternary deposits without back-filling. As shown in **Fig. 10**, the SPT N-values at the upper layer of medium sand with D_{50} of about 0.15 mm at Ohama No.1 Wharf are higher than those at Ohama No. 2 Wharf. As partly indicated by the SPT N-values shown at the levels higher than the present ground level, the level of the original ground surface had been a few meters higher than the present level. The grain size accumulation curves of sands at Ohama No. 1 Wharf are shown in **Fig. 11.**

If a comparison is made between the grain size accumulation curves of the sands at Ohama No. 2 Wharf, shown in **Fig. 7**, and those at Ohama No. 1 Wharf, shown in **Fig. 11**, the following observation can be made. The sand at the upper part of Ohama No. 1 Wharf has similar grain size accumulation curves as that of the backfill sand at Ohama No. 2 Wharf. Both of the sands are considered having the same origin, originally deposited from the Shinjo River. Similarly, the fine sands which constitute the lower sand layers at both of the wharves have the same grain size accumulation curves. Both of the sands are considered having the same origin, originally deposited from the Omono River.

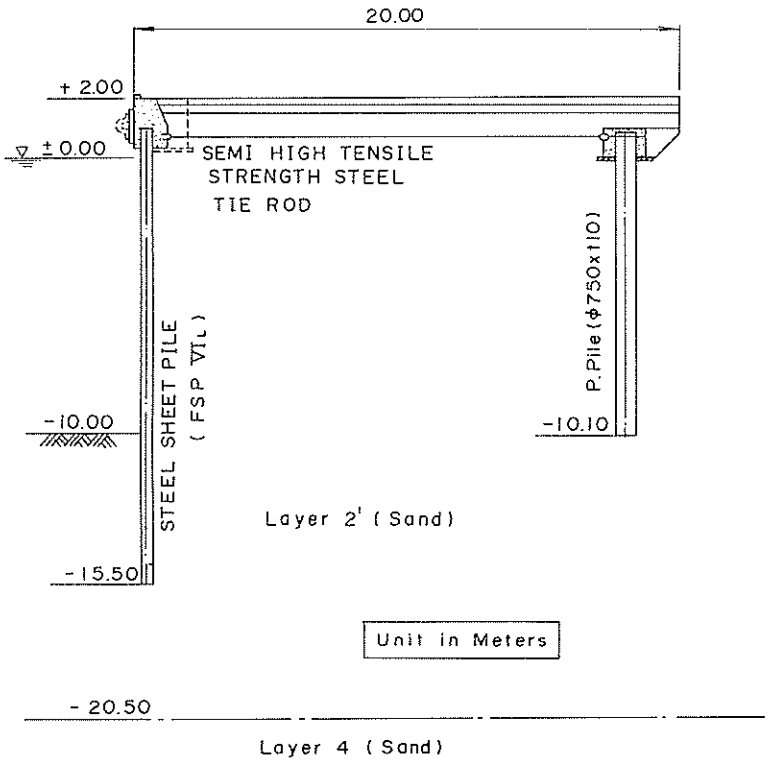

Fig. 9 Cross section of a quay wall at Ohama No. 1 Wharf

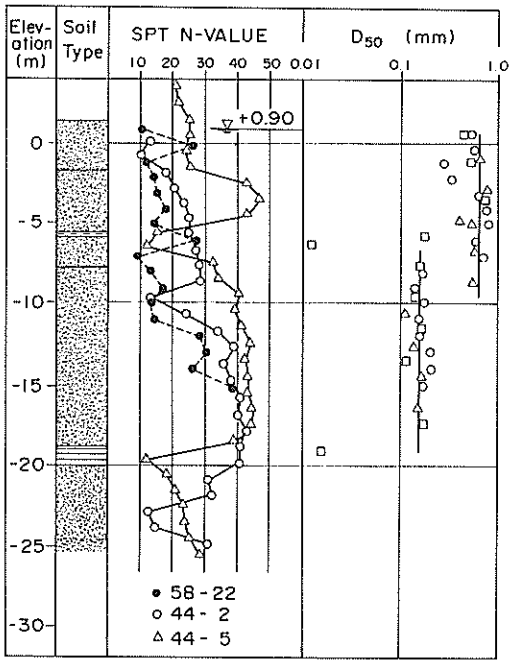

Fig. 10 Ground conditions at Ohama No. 1 Wharf

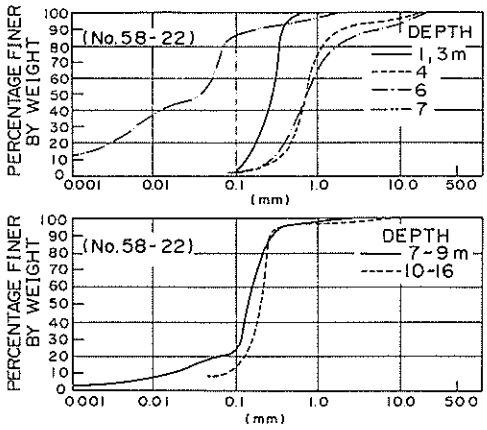

Fig. 11 Grain size accumulation curves of soils at Ohama No. 1 Wharf

To summarize, the sands at Ohama No. 1 Wharf are quite similar to those at Ohama No. 2 Wharf except for the SPT N-values of the upper part of the ground.

5. Liquefaction Resistance of Sands

In order to evaluate the liquefaction resistance of the sands constituting the upper and lower layers at Ohama No. 2 and No. 1 Wharves, two kinds of sands are taken from Akita Port. One is from the backfill at Ohama No. 2 Wharf, the other from the fill at Gaiko district, the location of which is shown at the upper left corner in **Fig. 1(c)**. The sand from Ohama No. 2 Wharf is considered representing the one constituting the upper sand layer at both of the Ohama Wharves because they are, as mentioned earlier, considered of the same origin. Similarly, the sand from Gaiko district is considered representing the one constituting the lower sand layer at both of the Ohama Wharves. The reason for this is that Gaiko district was constructed by filling the dredged sand from the nearby sea bottom at the estuary of the Omono River. Indeed, the grain size accumulation curve of the sand from Gaiko district is similar to that of the lower sand layer at both of the Ohama Wharves.

The undrained cyclic triaxial tests were conducted on the reconstituted samples of both of the sands. The results, plotted as the liquefaction resistance curves, are shown in **Fig. 12.** In this figure, the liquefaction resistance is defined referring to the states of (1) reaching the excess pore water pressure of 100% of the initial confining pressure as indicated by the open squares or circles and (2) reaching the axial strain level of 5% or 10% in the double amplitude as indicated by the closed squares, circles or triangles.

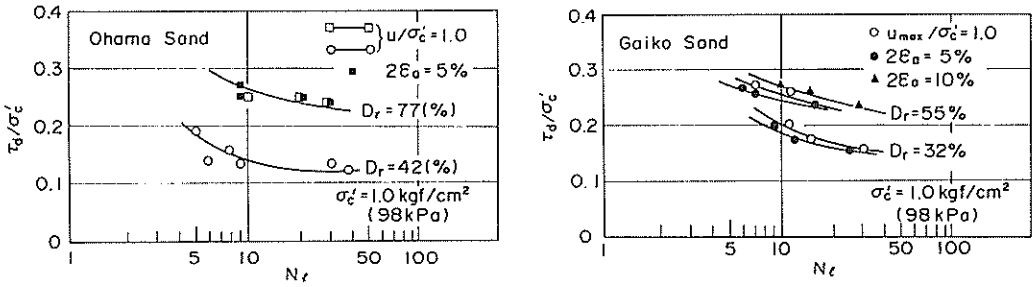

(a) Backfill sand at Ohama No. 2 Wharf (b) Fill sand at Gaiko district

Fig. 12 Liquefaction resistance curves of sands at upper and lower sand layers

6. Modeling of Soils

As partly mentioned earlier, the effective stress model of sands to be used in this study consists of a multiple shear mechanism (Iai et al., 1992a). With the effective stress and strain vectors written by

$$\{\sigma'\}^T = (\sigma_x' \ \sigma_y' \ \tau_{xy}) \tag{1}$$

$$\{\varepsilon\}^T = (\varepsilon_x \ \varepsilon_y \ \gamma_{xy}) \tag{2}$$

the basic form of the constitutive relation is given by

$$\{d\sigma'\} = [D](\{d\varepsilon\} - \{d\varepsilon_p\}) \tag{3}$$

in which

$$[D] = K\{n^{(\omega)}\}\{n^{(\omega)}\}^T + \Sigma R_{L/U}^{(i)}\{n^{(i)}\}\{n^{(i)}\}^T \tag{4}$$

In this relation, the term $\{d\varepsilon_p\}$ in **Eq. (3)** represents the additional strain increment vector to take the dilatancy into account and is given from the volumetric strain increment due to the dilatancy ε_p as

$$\{d\varepsilon_p\}^T = (d\varepsilon_p/2 \ d\varepsilon_p/2 \ 0) \tag{5}$$

The first term in **Eq. (4)** represents the volumetric mechanism with rebound modulus K and the direction vector is given by

$$\{n^{(\omega)}\}^T = (1 \ 1 \ 0) \tag{6}$$

The second term in **Eq. (4)** represents the multiple shear mechanism. Each mechanism $i = 1, \ldots, I$ represents a virtual simple shear mechanism, with each simple shear plane oriented at an angle $\theta_i/2 + \pi/4$ relative to the x axis. The tangential shear modulus $R_{L/U}^{(i)}$ represents the hyperbolic stress strain relationship with hysteresis characteristics. The direction vectors for the multiple shear mechanism in **Eq. (4)** are given by

$$\{n^{(i)}\}^T = \{\cos\theta_i \quad -\cos\theta_i \quad \sin\theta_i\} \quad (for\ i = 1, \ldots, I) \tag{7}$$

in which

$$\theta_i = (i - 1)\,\Delta\theta \quad (for\ i = 1, \ldots, I) \tag{8}$$

$$\Delta\theta = \pi / I \tag{9}$$

The loading and unloading for shear mechanism are separately defined for each mechanism by the sign of $\{n^{(i)}\}^T\{d\varepsilon\}$.

The multiple shear mechanism takes into account the effect of rotation of principal stress axis directions, the effect of which is known to play an important role in the cyclic behavior of the anisotropically consolidated sand (Iai et al., 1992b). The model has 10 parameters; two of which specify elastic properties of soil, another two specify plastic shear behavior, and the rest specify dilatancy.

In the present study, the parameters of the soils were determined from the in-situ velocity logging, the SPT N-values and the results of the undrained cyclic loading tests mentioned earlier. The details in determining the soil parameters are as follows.

In the analysis, the ground at Ohama No. 2 Wharf was idealized into four kinds of soil layers as indicated in **Fig. 4**. Similarly, the ground at Ohama No. 1 Wharf was idealized as indicated in **Fig. 9**. In this figure, the layer designated as Layer 2' is the combination of the upper and lower sand layers mentioned earlier. This was because the soil properties of both layers inferred from the SPT N-values were almost the same; when the SPT N-values of both layers shown in **Fig. 10** were corrected to the confining pressure of 1 kgf/cm² (98 kPa) as often done in the liquefaction potential evaluation (Seed et al., 1985), the corrected SPT N-values became almost uniform along the depth for both of the layers.

The elastic shear modulus G_{ma} was determined based on the in-situ velocity logging at Ohama No. 3 Wharf. The reference effective confining pressure of ($-\sigma_{ma}'$), which links the elastic modulus to the in-situ confining pressure in each soil layer, was determined with $K_0 = 0.5$ condition. The shear resistance angle ϕ_f' was determined by the triaxial test. The hysteretic damping factor at infinitely large shear strain H_m was determined to be 30% by referring to the typical laboratory results summarized by Ishihara (1982).

The rebound modulus of the soil skeleton K_a was determined by assuming that Poisson's ratio is 0.3. The phase transformation angle ϕ_p', which separates the dilative and contractive zones in the stress space, was assumed to be 30 degrees by referring to the typical laboratory results. The rest of the five parameters p_1, p_2, w_1, S_1 and c_1, which specify the dilatancy, were determined by the backfitting to the liquefaction resistance curves of the sand shown in **Fig. 13**. The liquefaction resistance curve for each layer shown in this figure was determined by combining the laboratory test data shown earlier and the SPT N-values at the sites for taking the in-situ conditions of soils into account. The procedures is given in the Appendix. More details of the backfitting procedure as well as the meaning of each parameter can be found in a paper by Iai et al. (1990).

The soil parameters determined in this manner are summarized in **Table 1**. An example is given in **Fig. 14** on the simulated cyclic behavior of the backfill sand computed by the present analytical model.

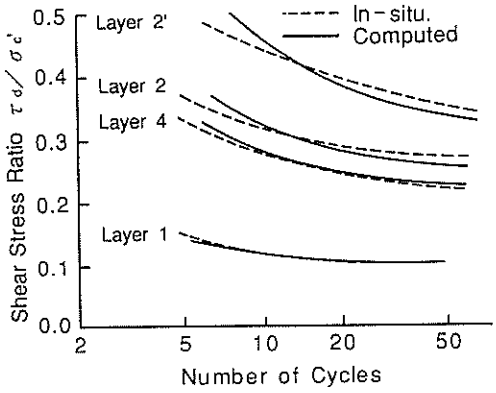

Fig. 13 In-situ and computed liquefaction resistance curves

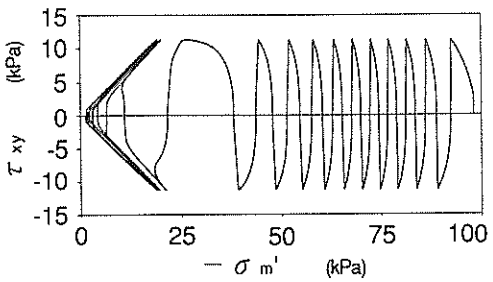

(a) Effective stress path

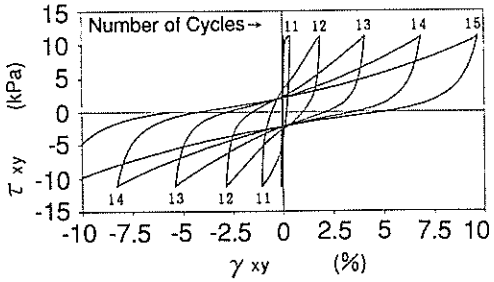

(b) Stress strain curve

Fig. 14 Computed results of cyclic simple shearing of soil at Layer 1

Table 1 Soil model parameters for the analysis

	Layer 1	Layer 2	Layer 2'	Layer 3	Layer 4
G_{ma} (kPa)	33800	72200	72200	74970	168200
K_a (kPa)	89930	192100	192100	199470	447530
$-\sigma_{ma}'$ (kPa)	50	110	60	140	157
ϕ_f (deg)	37	41	43	39	44
ϕ_p (deg)	30	30	30	—	30
S_1	0.005	0.005	0.005	—	0.005
W_1	0.5	8.5	14.0	—	3.8
p_1	0.4	0.5	0.5	—	0.5
p_2	0.42	0.8	1.0	—	0.84
c_1	1.5	3.3	4.6	—	2.4

Among the four soil layers idealized in the analysis, there exists a layer of clayey soil designated as Layer 3 in **Fig. 4**. The modeling of the clayey soil needs a slight modification in the present analytical model. The modification is in fact a simplification. The authors postulate in the present analysis that the clayey soil did not significantly change the effective mean stress during the earthquake shaking and, as an approximation, kept the initial effective mean stress being constant throughout the shaking. This might be a crude approximation for a realistic behavior of the clayey soil. As a compensation, the effective angle of shear resistance of the clayey soil was so determined as to give the same undrained shear strength as measured in the laboratory with the unconfined undrained compression tests.

7. Modeling of Structures and Sea Water

The quay walls at Ohama No. 1 and No. 2 Wharves had the same type of sheet piles as mentioned earlier. The sheet piles forming the quay walls were type FSP-VI_L manufactured in Japan, having the following properties; the second moment of area 8.6 $\times 10^{-4}$ m^4, cross sectional area 0.0306 m^2, and density 7.5 t/m^3 (each specified per unit breadth of the beam). In the analysis, the sheet piles were simulated with linear beam elements. It is known that the displacement shape functions assumed in the commonly used beam element (e.g. Zienkiewicz, 1977) are incompatible with those of the isoparametric solid element representing the soil and hence pose a potential threat to cause an undesirable effect on the computed results of the soil-structure interaction. In the present study, more appropriate beam elements were used of which displacement shape functions are exactly compatible with those of the solid element (Hinton and Owen, 1977).

No friction was assumed to be acting between the soil and the sheet pile wall. This assumption was implemented in the analysis by imposing such a condition that the displacements of the nodal points of the soil elements and the beam elements be the same with each other in the horizontal direction but can take independent values in the vertical direction.

The tie rod was simulated by a linear beam element, mass of which was assumed to be zero, and was connected with the sheet pile and the anchor piles by hinges. No interaction was taken into account between the soil and the tie rod. This was implemented in the analysis by simply specifying the geometry of the beam element without any connection with the soil elements.

The anchor piles were idealized also by the linear beam elements. In particular, two rows of the anchor piles at Ohama No. 2 Wharf were idealized by the linear beam elements, top ends of which were rigidly fixed with each other for simulating the upper concrete structure of the anchor. No friction was assumed to be acting between the soil and the anchor piles. The numerical implementation of this was done in a similar manner as mentioned earlier.

The sea water was modeled as incompressible fluid and was formulated as an added mass matrix based on the equilibrium and continuity of the fluid at the solid-fluid interface (Zienkiewicz, 1977).

8. Initial and Boundary Conditions

8.1 Initial Conditions

Before the earthquake response analysis, a static analysis was conducted with gravity to simulate the initial stresses acting in-situ before the earthquake. The same constitutive model was used as in the earthquake response analysis but with the drained condition.

Obviously a more realistic static analysis could be done by closely simulating the actual steps taken in the construction of the structures; i.e. by simulating the processes of the pile driving and the backfilling or the excavation and, if any, the effect of the pre-stress histories in the ground due to the previous earthquakes. These steps, if taken, will be so complicated that the static analysis itself can become a major research problem. In the present analysis, such a complication was avoided because the main target was on the earthquake response analysis. The authors assumed that a simple one step loading of gravity will give a reasonable approximation of the initial stress condition. The initial earth pressures and bending moments obtained as the initial conditions will be shown later with the results of the dynamic response analysis.

8.2 Boundary Conditions

During the earthquake response analysis, the seismic waves should be appropriately permitted to transmit from the domain of the analysis with the finite elements to the outside field because the boundaries of the domain fixed for the analysis do not exist in reality. In order to take this fact into account in an approximate manner, the side and bottom boundaries of the domain were simulated by viscous dampers.

The dynamic analysis should also appropriately take into account the effect of the earthquake waves transmitted from the outside field. In the present analysis, the incident wave transmitted vertically from the bottom boundary was given through the viscous dampers at the bottom. The effects of the free field motions, simulated by the one dimensional responses at outside fields, were also taken into account by transmitting them through the viscous dampers at both sides of the boundaries.

9. Input Motion and Time Integration

With these initial and boundary conditions, the earthquake response analysis was conducted on the steel sheet pile quay walls at Akita Port. As an input motion, both of the horizontal components of the earthquake motion recorded at Akita Port, shown in **Fig. 3**, were at first deconvoluted by the equivalent linear method for obtaining the incident waves, and transformed into the components normal to the faces of the quay walls.

The dynamic analysis of the quay walls was conducted under the undrained conditions (Zienkiewicz et al., 1982). The numerical integration was done by the Wilson-θ method ($\theta = 1.4$) using a time step of 0.01 seconds. Rayleigh damping ($\alpha = 0$ and $\beta = 0.005$) which was proportionally decreasing with the degree of cyclic mobility was used to ensure stability of the numerical solution process.

10. Analysis of a Damaged Quay Wall

10.1 Earthquake Response and Deformation

The effective stress analysis of the quay wall at Ohama No. 2 Wharf resulted in the deformation shown in **Fig. 15**; deformations towards the sea are mainly seen at the soils in front of and behind the sheet pile wall.

The maximum acceleration at the top of the quay wall was about 190 Gals as shown in the second row in **Fig. 16(a)**. In this figure and the figures to follow, the alphabets indicate the locations shown in **Fig. 15**. As the shaking continues, the horizontal displacements gradually increased towards the sea as shown in **Fig. 16(b)**. The backfill soil behind the sheet pile wall gradually settled as shown in the lower two rows in **Fig. 16(c)** whereas the sea bed in front of the sheet pile wall gradually swelled as shown in the top row in the same figure.

The horizontal displacement at the top of the sheet pile wall was computed being about 1.3 m at the end of the shaking whereas the observed displacements range, as mentioned earlier, from about 1.1 to 1.8 meters, indicating the computed displacement is consistent with those observed.

The settlements behind the sheet pile wall were computed being about 0.7 meters at the end of the shaking whereas the observed settlements, as mentioned earlier, were about 1.4 meters. Should the effect of yielding of the sheet pile be included in the analysis, the computed settlements would be greater and closer to those observed.

10.2 Earth Pressure and Bending Moment

As shown in **Fig. 17**, the earth pressures (i.e. the summations of the normal effective stresses and the excess pore water pressures) acting on the sheet pile wall became greater than those before the shaking. In particular, the earth pressures behind the sheet pile after the shaking became about the same as those with the earth pressure coefficient of K_0 = 1.0. This is consistent with the results of the previous

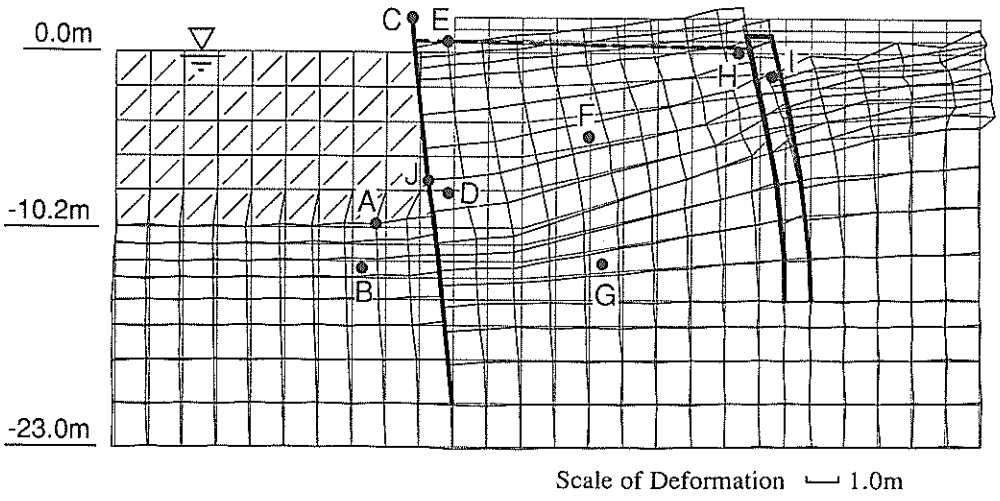

Fig. 15 Computed deformation of a quay wall at Ohama No. 2 Wharf at 30 seconds of shaking

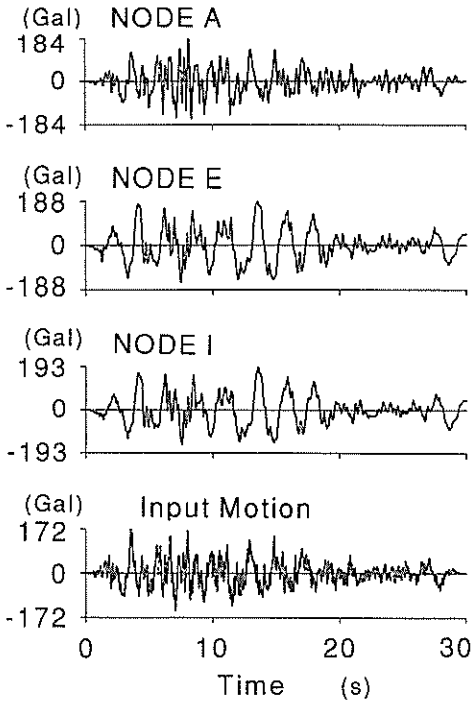

(a) Horizontal accelerations

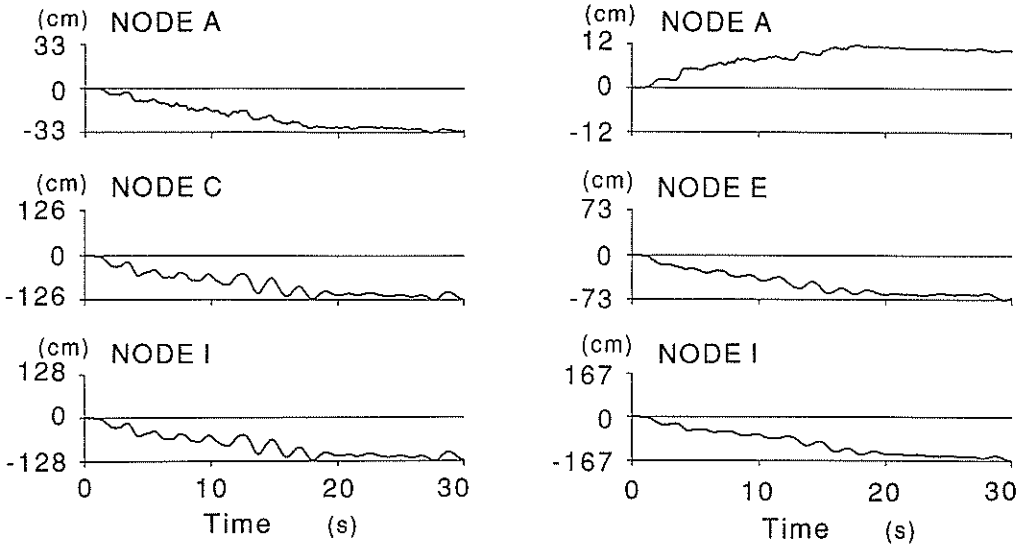

(a) Horizontal displacements

(c) Vertical displacements

Fig. 16 Computed response accelerations and displacements at Ohama No. 2 Wharf

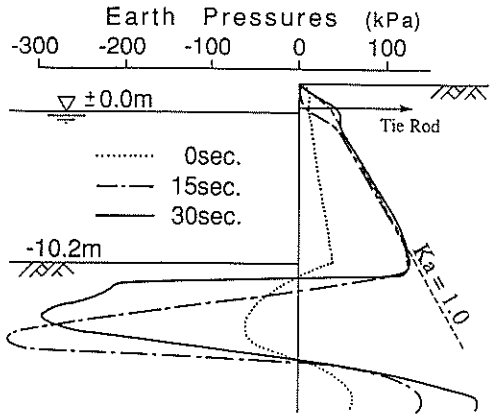

Fig. 17 Earth pressures on a quay wall at Ohama No. 2 Wharf

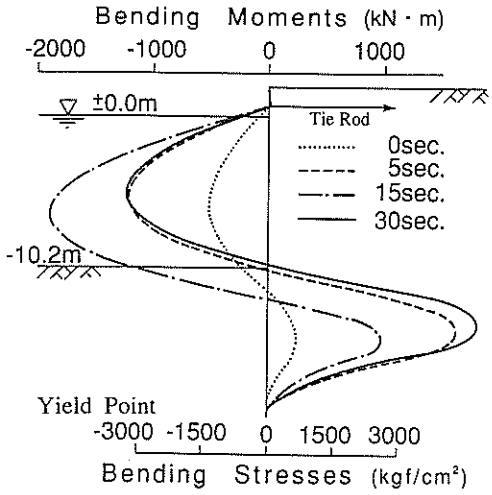

Fig. 18 Bending moments and bending stresses of a sheet pile at Ohama No. 2 Wharf (1 kgf/cm² = 98 kPa)

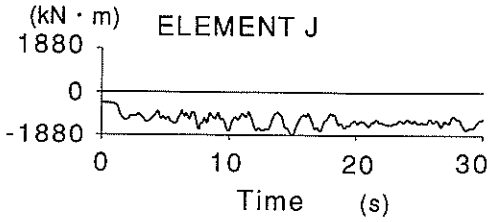

Fig. 19 Time history of bending moment of a sheet pile at the elevation of -6 m at Ohama No. 2 Wharf

laboratory study on the earth pressures acting on the fixed wall due to the liquefied soil (Tsuchida, 1968).

In accordance with those changes in the earth pressures, the bending moment of the sheet pile became greater as shown in **Fig. 18**. In particular, the bending moment at the level of 6 meters below the sea water level gradually increased as shown in **Fig. 19**.

As shown in **Fig. 18**, the maximum stress due to bending was computed as 500000 kPa whereas the yield strength of the steel sheet pile is 300000 kPa (1 kgf/cm² = 98 kPa). This indicates that the observed phenomenon, i.e. the failure of the sheet pile, is well explained by the present analysis because, as mentioned earlier, the sheet pile was idealized in the analysis with the linear beam elements, which were assumed never to fail.

The analysis also indicates some possibility of yielding below the sea bottom. In Akita Port, a sheet pile was pulled out from the ground after the earthquake, revealing the opening of a crack at the level of 2.2 meters below the sea bottom. This is consistent with the results of the analysis. The excess pore water pressures in the soils in front of and behind the sheet pile wall were computed as shown in **Fig. 20**.

The excess pore water pressures rapidly increased behind the sheet pile wall at

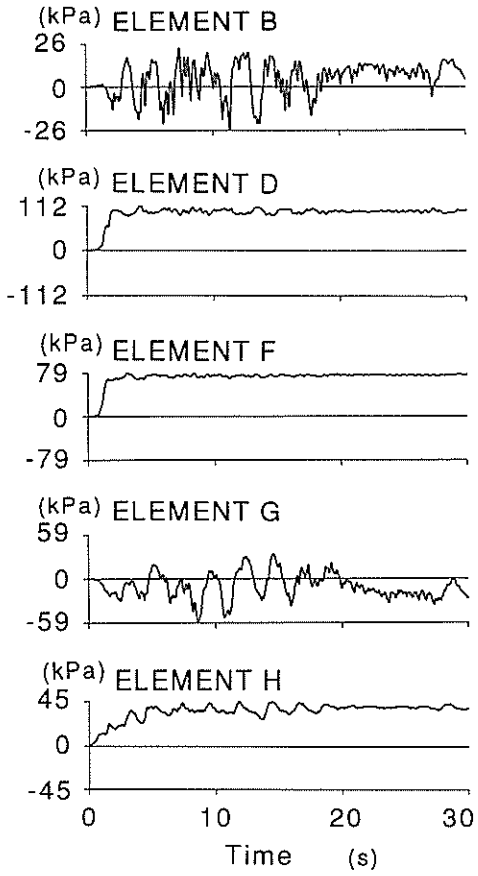

Fig. 20 Excess pore water pressures at Ohama No. 2 Wharf

the initiation of the shaking as shown in the second and third rows. The excess pore water pressures in front of the sheet pile wall, however, fluctuated around the value of zero as shown in the top row in **Fig. 20** possibly because of the high liquefaction resistance of the soil.

11. Analysis of an Undamaged Quay Wall

11.1 Earthquake Response and Deformation

The effective stress analysis of the quay wall at Ohama No. 1 Wharf resulted in the deformation shown in **Fig. 21**. The maximum acceleration at the top of the quay wall was about 270 Gals as shown in the second row in **Fig. 22(a)**, being much higher than in the case of Ohama No. 2 Wharf, but the horizontal displacement, shown in the second row in **Fig. 22(b)**, was only about 0.2 m. The observed displacement at Ohama No. 1 Wharf was about 0.05 m, indicating the analysis provided a slightly conservative result, erring in the order of 0.1~0.2 m.

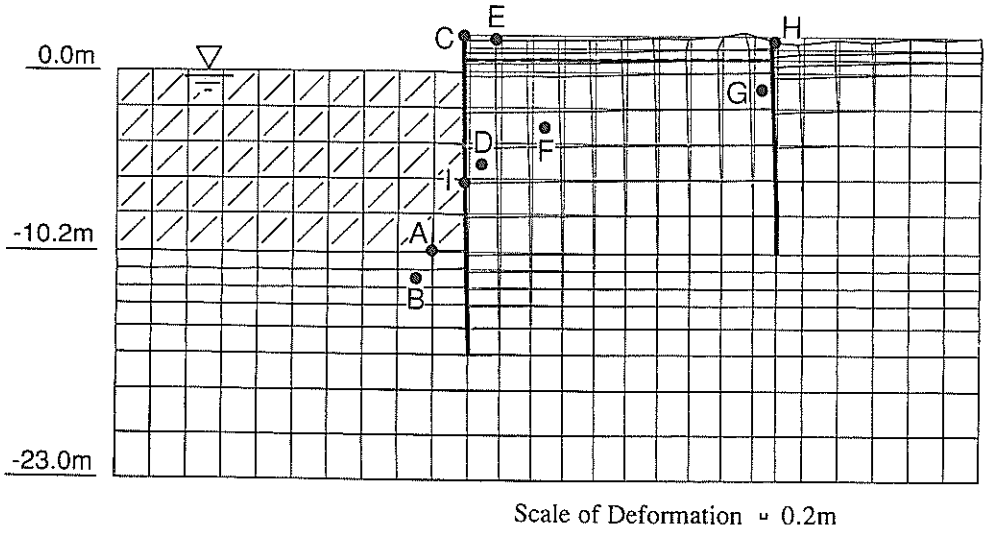

Fig. 21 Computed deformation of a quay wall at Ohama No. 1 Wharf at 30 seconds of shaking

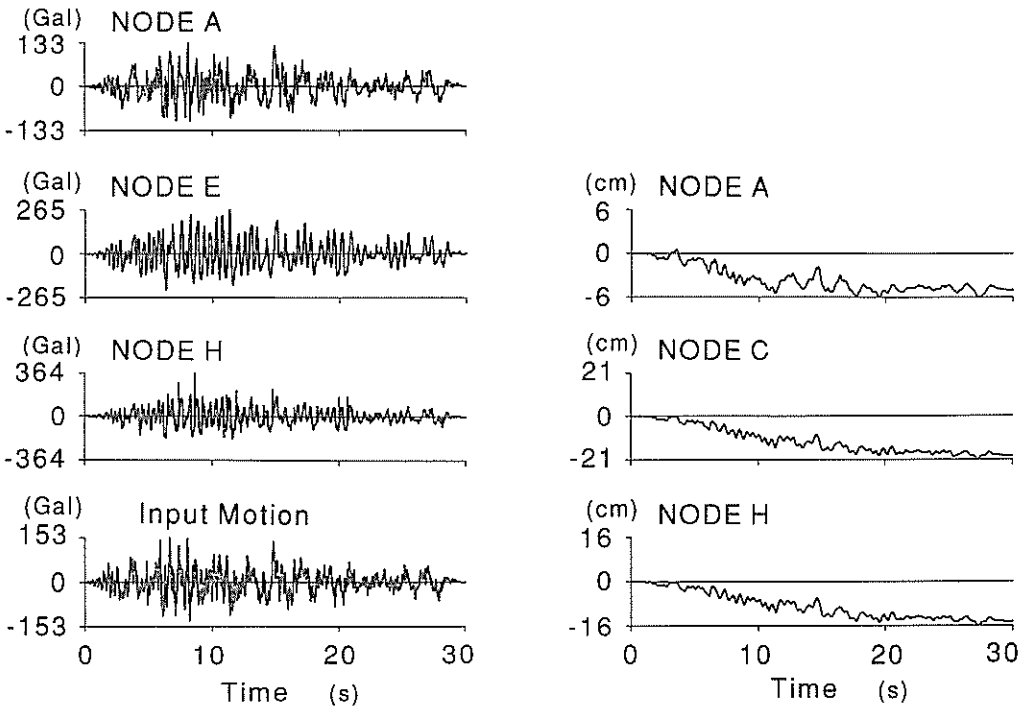

(a) Horizontal accelerations (c) Horizontal displacements

Fig. 22 Computed response accelerations and displacements at Ohama No. 2 Wharf

11.2 Earth Pressure and Bending Moment

As shown in **Fig. 23**, the earth pressures acting on the sheet pile wall became greater than those before the shaking. In particular, those behind the sheet pile wall became close to those with K_0 = 1.0 condition from the ground surface to the elevation of about five meters below the sea water level, but at the lower levels the earth pressures remained very much smaller than those with K_0 = 1.0 condition.

In accordance with those changes in the earth pressures, the bending moment of the sheet pile changed as shown in **Fig. 24**. In particular, the bending moment at the level of 6 meters below the sea water level gradually increased as shown in **Fig. 25**. The maximum stress due to bending was computed as 300000 kPa as shown in **Fig. 24** whereas the yield strength of the steel sheet pile is also 300000 kPa, indicating that the analysis provided a slightly conservative result.

The excess pore water pressures in the soils in front of and behind the sheet pile wall were computed as shown in **Fig. 26**. The excess pore water pressures gradually increased behind the sheet pile wall as the shaking continued as shown in the second and third rows, but never so rapidly as in the case of Ohama No. 2 Wharf. The excess pore water pressures in front of the sheet pile wall remained fluctuating around the value of zero as shown in the top row in **Fig. 26**.

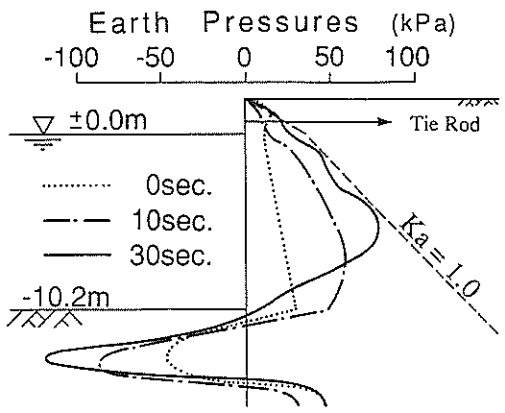

Fig. 23 Earth pressures on a quay wall at Ohama No. 1 Wharf

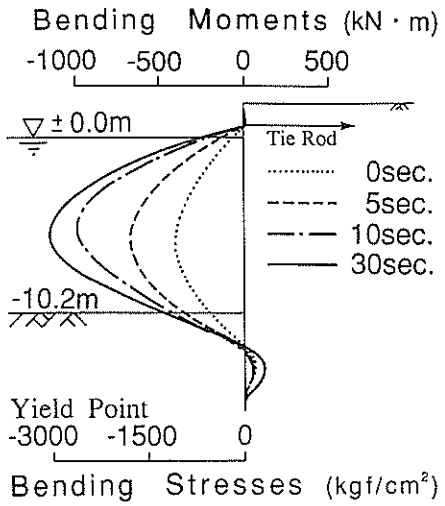

Fig. 24 Bending moments and bending stresses of a sheet pile at Ohama No. 1 Wharf (1 kgf/cm² = 98 kPa)

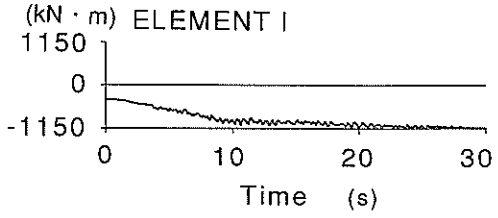

Fig. 25 Time history of bending moment of a sheet pile at the elevation of -6 at Ohama No. 1 Wharf

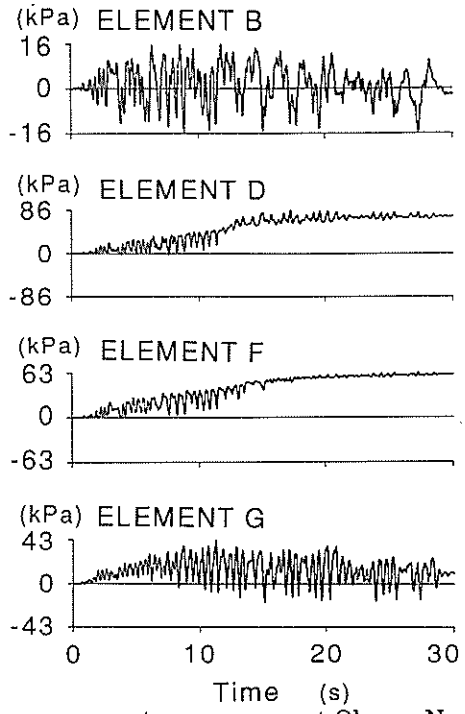

Fig. 26 Excess pore water pressures at Ohama No. 1 Wharf

12. Mechanism of Deformation

In order to look into the mechanism of deformation of the quay walls, the stress and strain of soils in front of and behind the damaged sheet pile wall, indicated by B and D in **Fig. 15**, are plotted in **Fig. 27**. The stress and strain notations are defined as extension being positive.

In front of the sheet pile, the effective stress path, plotted as a relationship between the deviatoric stress $\tau = -(\sigma_1' - \sigma_3')/2$ and the effective mean stress $(-\sigma_m') = -(\sigma_1' + \sigma_3')/2$ in the upper most row in **Fig. 27(a)**, gradually approaches the failure line with fluctuation around the initial deviatoric stress. In accordance with this, the axial strain difference is gradually induced as shown in the middle row in the same figure. The shear strain γ_{xy} is also gradually induced in accordance with the inclination of the sheet pile but the magnitude of the shear strain is relatively small as shown in the bottom row in the same figure.

Behind the sheet pile wall, the effective mean stress $(-\sigma_m')$ rapidly decreases as shown in the upper most row in **Fig. 27(b)**. In accordance with this, the axial strain difference is gradually induced as shown in the middle row in the same figure. The magnitude of the shear strain γ_{xy} in the soil behind the sheet pile wall is relatively small as shown in the bottom row in the same figure.

To summarize, deformations of quay walls are likely to be induced due to the existence of initial stress and its release in accordance with overall softening of saturated soil with the mechanism of cyclic mobility. This mechanism of deformation is quite different from the mechanism of the sliding blocks, which are generally observed in dry sands.

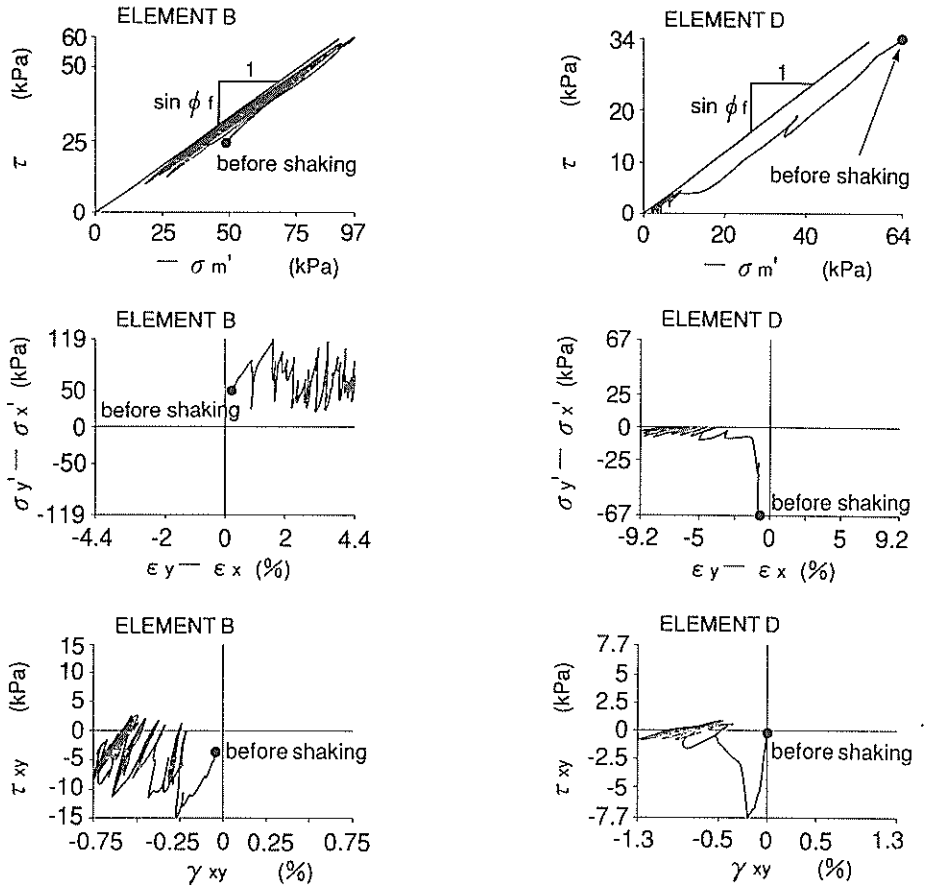

(a) In front of the sheet pile (c) Behind the sheet pile

Fig. 27 Stress and strain in soil at Ohama No. 2 Wharf

13. Discussions

Despite the certain agreement between the computed and observed performance of the quay walls with the reasonable mechanism for explaining the deformation, it would not be easy to jump to the conclusion that the applicability of the present effective stress model is confirmed without reservation. Before arriving at definite conclusions, the approximations and the assumptions made through the course of the analysis may have to be put under scrutiny. The major approximations and the assumptions made in the present study are

(1) simulating the initial stress conditions by the single step gravity analysis,
(2) imposing the undrained conditions on the sand,
(3) assuming no frictions between the soil and the structures,
(4) representing the two or three dimensional earthquake motion by one horizontal component normal to the face of the quay wall, and
(5) simulating the anchor piles by the beam elements in the two dimensional analysis.

Those listed in (2) and (3) will cause conservative results (i.e. larger displacements, larger bending moments, etc.) whereas those in (4) and (5) will cause unconservative results (i.e. smaller displacements, etc). The one listed in (1) may cause either conservative or unconservative results depending on the in-situ stress conditions. Thus, it would not be easy to determine whether these factors, as a whole, will cause conservative or unconservative errors.

Obviously the ultimate goal of the validation of the effective stress model will only be achieved through the rigorous estimation on the overall effects of those approximations and assumptions. It might as well be said that the efforts for this will require some years and result in several technical papers, each dealing with an important problem in geotechnical and earthquake engineering. Then, a critical question may have to be answered as to exactly what can be learned from the present study.

The present study is one of those early attempts being in its infancy to broaden our prospects on the capability of the effective stress analysis. Though the exact magnitude of deformation may be affected by such factors listed earlier, difference between the deformations of the two quay walls, especially the order-of-magnitude difference between them, will not be very much affected by those factors; if a factor increases the deformation in one quay wall, it will increase the deformation in the other quay wall as well. The only exception may be the initial conditions. However, the past experiences in ports during earthquakes taught us that extensive soil liquefaction very often causes serious damage to the quay walls no matter what type of structures were involved or what kind of initial conditions existed. Consequently, it would be possible to draw the conclusion that the present analytical model has the potential ability to differentiate between serious large deformations (i.e. damage) from negligible small deformations (i.e. no damage) in similar types of sheet pile quay walls during an earthquake.

As an example of the application of the present approach, effect of the liquefaction resistance of backfill sand is studied in relation to the maximum bending moment of the sheet pile induced by the earthquake shaking. The quay wall at Ohama No. 2 Wharf is taken as an example. The liquefaction resistances of the backfill sand are varied as shown in **Fig. 28**. The maximum bending moment, which exceeded the yield point when the backfill sand was very loose as in the actual earthquake, becomes smaller if the

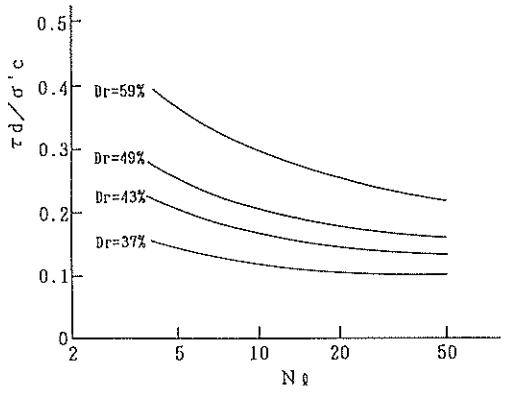

Fig. 28 Varied liquefaction resistance of backfill soil

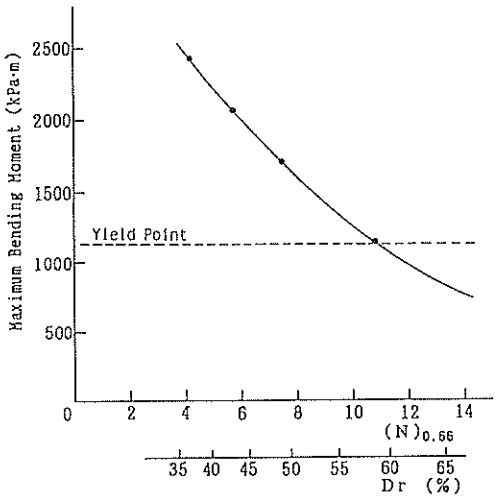

Fig. 29 Relation between the maximum bending moment of sheet pile and the relative density of backfill soil at Ohama No. 2 Wharf

liquefaction resistance of the backfill sand is increased as shown in **Fig. 29**. This type of analysis may be useful in design when the backfill sand should be improved as a measure against liquefaction.

14. Summary and Conclusions

A two dimensional effective stress analysis was conducted on the behavior of the sheet pile quay walls. The results of the analysis were consistent with the observed performance of the damaged and undamaged quay walls. In the analysis, major deformations were seen in the soils in front of and behind the sheet pile wall. In both of the soils, the strains were gradually induced due to the existence of initial stress and its release in accordance with overall softening of soil with the mechanism of cyclic mobility.

With the reasonable mechanism available for explaining the deformation of sheet pile quay walls, the authors conclude that the present model has the potential ability to differentiate between serious large deformations (i.e. damage) and very small deformations (i.e. no damage) in similar types of sheet pile quay walls.

Acknowledgments

The authors wish to thank Professors K. Ishihara and I. Towhata at Tokyo University for their valuable discussions and encouragement.

References

1) HINTON, E. and OWEN, D.R.J., (1977): Finite Element Programming, *Academic Press*, p. 305.
2) IAI, S., KURATA, E. and TSUCHIDA, H., (1978): "Digitization and correction of strong-motion accelerograms," *Technical Note of the Port and Harbour Research Institute*, No. 286, p. 56 (in Japanese).
3) IAI, S., TSUCHIDA, H. and KOIZUMI, K., (1989): "A liquefaction criterion based on field performances around seismograph stations," *Soils and Foundations*, Vol. 29, No. 2, pp. 52~68.
4) IAI, S., MATSUNAGA, Y. and KAMEOKA, T., (1990): "Parameter identification for a cyclic mobility model," *Report of the Port and Harbour Research Institute*, Vol. 29, No. 4, pp. 57~83.
5) IAI, S., MATSUNAGA, Y. and KAMEOKA, T., (1992a): "Strain space plasticity model for cyclic mobility," *Soils and Foundations*, Vol. 32, No. 2, pp. 1~15.
6) IAI, S., MATSUNAGA, Y. and KAMEOKA, T., (1992b): "Analysis of undrained cyclic behavior of sand under anisotropic consolidation," *Soils and Foundations*, Vol. 32, No. 2, pp. 16~20.
7) ISHIHARA, K., (1982): "Evaluation of soil properties for use in earthquake response analysis," *Proceedings of International Symposium on Numerical Models in Geomechanics*, Zurich, pp. 237~259.
8) KANO, T., (1965): "On the topography and quaternary geology in the north area of Akita City, Akita Prefecture, Northeast Honshu," *Report of the Research Institute of Underground Resources*, Mining College, Akita University, No. 33, pp. 1~12 (in Japanese).
9) KURATA, E. and IAI, S., (1990): "Annual report of strong-motion earthquake records in Japanese ports (1989)," *Technical Note of the Port and Harbour Research Institute*, No. 676, p. 324.
10) KURATA, E., FUKUHARA, T. and NODA, S., (1983): "Strong-motion earthquake records on the 1983 Nipponkai-Chubu Earthquake in port areas," *Technical Note of the Port and Harbour Research Institute*, No. 458, p. 372.
11) Ministry of Transport (1965): "Damage to port structures by the Niigata Earthquake of 1964," p. 249.
12) SEED, H.B., TOKIMATSU, K., HARDER, L.F. and CHUNG, R.M., (1985): "Influence of SPT procedures in soil liquefaction resistance evaluations," *Journal of Geotechnical Engineering Division*, ASCE, Vol. 111, No. 12, pp. 1425~1445.
13) TOKIMATSU, K. and YOSHIMI, Y., (1983): "Empirical correlation of soil liquefaction based on SPT N-value and fines content," *Soils and Foundations*, Vol. 23, No. 4, pp. 56~74.
14) TOWHATA, I. and ISLAM, M.S., (1987): "Prediction of lateral displacement of anchored bulkheads induced by seismic liquefaction," *Soils and Foundations*, Vol. 27, No. 4, pp. 137~147.
15) TSUCHIDA, H., (1968): "Earth pressure due to liquefied soil," *Tsuchi-to-Kiso*, Japanese Society of Soil Mechanics and Foundation Engineering, Vol. 16, No. 5, pp. 3~10 (in Japanese).
16) TSUCHIDA, H., NODA, S., INATOMI, T., UWABE, T., IAI, S., ONEDA, H. and TOYAMA, S., (1985): "Damage to port structures by the 1983 Nipponkai-Chubu Earthquake," *Technical Note of the Port and Harbour Research Institute*, No.

511, p. 447 (in Japanese).

17) WHITMAN, R.V., (1991): "Seismic design of earth retaining structures (state of the art paper)," *Proceedings of the Second International Conference on Recent Advances in Geotechnical Earthquake Engineering and Soil Dynamics*, St. Louis, Vol. 2, pp. 1767~1778.

18) YOSHIMI, Y., TOKIMATSU, K. and HOSAKA, Y., (1989): "Evaluation of liquefaction resistance of clean sands based on high-quality undisturbed samples," *Soils and Foundations*, Vol. 29, No. 1, pp. 93~104.

19) ZIENKIEWICZ, O.C., (1977): The Finite Element Method, 3rd edition, *McGraw-Hill Book Co.*

20) ZIENKIEWICZ, O.C. and BETTESS, P., (1982): "Soils and other saturated media under transient, dynamic conditions," *Soil Mechanics — Transient and Cyclic Loads* (Pande and Zienkiewicz eds.), John Wiley and Sons, pp. 1~16.

Appendix

The in-situ liquefaction resistance of sands is known to be difficult to evaluate from the laboratory test results of reconstituted samples but might better be evaluated from the SPT N-values (Yoshimi et al., 1989). In the present study, the liquefaction resistance of the backfill sand in Layer 1 at Ohama No. 2 Wharf, being hydraulically filled about seven years before the earthquake, was evaluated from the laboratory test results on the reconstituted samples. Other layers were of alluvial or diluvial origin and hence the liquefaction resistance was evaluated from the SPT N-values. Though, in early days, there had been a discrepancy among the field correlations obtained by several researchers, the recent studies conducted by Tokimatsu and Yoshimi (1983), Seed et al., (1985) and one of the authors and his colleagues agree quite well among themselves (Iai et al., 1989). In particular, the liquefaction resistance level referring to the state reaching axial strain level of 5% in the double amplitude inferred from the correlation by Seed et al. (1985) fits very well with those referring to the state of F_l = 1.0 in the correlation by Iai et al. (1989). In the present study, this level of the liquefaction resistance was used for evaluating the level of the in-situ liquefaction resistance for the sand layers of alluvial or diluvial origin.